Revista Internacional de Contaminación Ambiental
ISSN: 0188-4999
rvp@atmosfera.unam.mx
Universidad Nacional Autónoma de México
México

CHARACTERIZATION AND SURFACE REACTIVITY OF NATURAL AND SYNTHETIC MAGNETITES: II. ADSORPTION OF Pb(II) AND Zn(II)

Salazar Camacho, Carlos Adolfo; Villalobos Peñalosa, Mario
CHARACTERIZATION AND SURFACE REACTIVITY OF NATURAL AND SYNTHETIC MAGNETITES: II. ADSORPTION OF Pb(II) AND Zn(II)
Revista Internacional de Contaminación Ambiental, vol. 33, no. 1, 2017
Universidad Nacional Autónoma de México, México
Available in: http://www.redalyc.org/articulo.oa?id=37050971016
DOI: http://dx.doi.org/10.20937/RICA.2017.33.01.15

CHARACTERIZATION AND SURFACE REACTIVITY OF NATURAL AND SYNTHETIC MAGNETITES: II. ADSORPTION OF Pb(II) AND Zn(II)

CARACTERIZACIÓN Y REACTIVIDAD SUPERFICIAL DE MAGNETITAS NATURALES Y SINTÉTICAS: II. ADSORCIÓN DE Pb(II) Y Zn(II)

Carlos Adolfo Salazar Camacho, *Facultad de Ciencias Naturales, Departamento de Biología, Universidad Tecnológica del Chocó, Colombia*, casaca31@hotmail.com

Mario Villalobos Peñalosa, *Laboratorio de Geoquímica Ambiental, Departamento de Geoquímica, Instituto de Geología, Universidad Nacional Autónoma de México, México*

DOI: http://dx.doi.org/10.20937/RICA.2017.33.01.15
Redalyc: http://www.redalyc.org/articulo.oa?id=37050971016

Received: 01 January 2016
Accepted: 01 May 2016

Abstract

Two synthetic and three natural magnetite samples that were obtained from an iron ore deposit located in Central-Western Mexico, were used to investigate the magnetite surface reactivity of different particle sizes towards aqueous Pb(II) and Zn(II). From these, the synthetic samples < 50 nm [specific surface area (SSA)] = 39.3 m^2 /g), < 5 mm (SSA = 7.3 m2/g), and natural samples 948-fine (SSA = 7.6 m^2 /g), 948 (SSA = 3.0 m^2 /g) and 996 (SSA = 1.4 m^2 /g), successfully removed Pb(II) from aqueous solutions at the investigated pH value of 5.8, but only the three first, finer magnetites removed significant aqueous Zn(II) at pH 7.0. The adsorption kinetics data were fitted using pseudo-second order and intraparticle models. The Pb(II) adsorption capacities were 140.1, 33.3, 65.4, 69.8 and 17.0 mmol/g, for samples < 50 nm, < 5 mm, 948-fine, 948 and 996, respectively, while for Zn(II) they were 159.2, 38.8 and 28.2 mmol/g, for the first three previous samples, respectively. These adsorption capacities suggest that magnetite may play an important role as adsorbents of cationic contaminants in the environment, or that it may be used as efficient remediating agent, but it's limited to particle sizes with specific surface areas above 3 m^2 /g.

Keywords: kinetics, metals, removal, aggregation, nanoparticles, iron oxides.

Resumen

Dos muestras de magnetita sintética y tres naturales, que fueron obtenidas de un yacimiento minero ubicado en el centro-occidente de México, se utilizaron para investigar la reactividad superficial de magnetitas de diferentes tamaños de partícula hacia Pb(II) y Zn(II). Los resultados mostraron que las magnetitas sintéticas < 50 nm [área superficial específica (ASE)] = 39.3 m^2 /g), < 5 mm (ASE = 7.3 m^2 /g), y las naturales 948-fina (ASE = 7.6 m^2 /g), 948 (ASE = 3.0 m^2 /g) y 996 (ASE = 1.4 m^2 /g), removieron exitosamente Pb(II) en disolución acuosa al pH investigado de 5.8, pero sólo las primeras tres magnetitas más finas removieron significativamene también Zn(II) acuoso a pH 7.0. Los datos de cinética de adsorción se ajustaron utilizando los modelos de pseudosegundo orden y difusión intrapartícula. Las capacidades de adsorción para Pb(II) fueron de 140.1, 33.3, 65.4, 69.8 y 17.0 mmol/g, para las muestras < 50 nm, < 5 mm, 948-fina, 948 y 996, respectivamente. Mientras que para Zn(II) fueron 159.2, 38.8 y 28.2 mmol/g, para las tres primeras anteriores, respectivamente. Estos valores de capacidad de retención sugieren que la magnetita puede desempeñar un papel importante como adsorbente de contaminantes catiónicos en el ambiente, o puede ser utilizada como adsorbente eficiente en esquemas de remediación, pero está limitada a tamaños de partícula de áreas superficiales específicas por arriba de 3 m^2 /g.

Palabras clave: cinética, metales, remoción, agregación, nanopartículas, óxidos de hierro.

Author notes

casaca31@hotmail.com

INTRODUCTION

Heavy metals such as Pb, Zn, Cu, Hg and Cd reach geochemical environments as a result of anthropogenic activities including smelting, mining and manufacturing industries, and may become mobile under oxic conditions and thus bioavailable. The health risks posed to biota from heavy metals is high because they are not chemically and biologically degradable, so they will remain in the environment after disposal. Additionally, their concentrations in higher organisms may increase via the trophic chain, especially causing health problems in humans (Trivedi and Axe 2000, ATSDR 2005, 2012, USEPA 2007, Sánchez et al. 2013). In order to comply with the guidelines of environmental regulatory agencies, various methodologies have been employed to remove metal ions from aqueous contaminated environments. These methods include coagulation, precipitation, ion exchange processes, adsorption on activated carbon, organic based extraction, electrochemical treatments and biosorption processes (Atar et al. 2012, Mudhoo et al. 2012). However, these methods may show drawbacks such as high capital and operating costs, and the need to dispose metal bearing sludge and secondary wastes (Wang et al. 2014).

In natural systems, the availability of metal ions is partly controlled by adsorption processes that occur on the surfaces of mineral particles of small sizes. When these adsorbent minerals are not naturally present or are insufficient in contaminated environments, the use of synthetic mineral amendments becomes necessary for immobilization purposes. In this manner, nanocomposites of clays and iron oxides (such as zeolites and montmorillonite functionalized with zero-valent iron (nZVI) and maghemite), and colloidal and nanoparticulate metal oxides, have been adopted as useful and economical materials for removing (through sorption processes) metal ions such as Pb(II), Co(II), Ni(II), Cd(II), Zn(II) and Cr(VI) from contaminated environments (Bargar et al. 1997, 1998, Waychunas et al. 2002, Tani et al. 2004, Villalobos et al. 2005, Uheida et al. 2006, Barquist and Larsen 2010, Hua et al. 2012, Wang et al. 2014, Arancibia et al. 2016, Kong et al. 2016).

Among the metal oxides used, the iron oxide magnetite has proven useful for removing ions from polluted environments, especially from water and wastewater (Nassar 2010, Wang et al. 2011, Giraldo et al. 2013), but very limited work has been reported using natural magnetites. When applied to contaminated heterogeneous media, magnetite has the added potential advantage of magnetic separation from the solid matrix after adsorbing the target pollutants. Nevertheless, synthetic nanomagnetites have been studied more frequently as sorbents, because of their high adsorption capacities (Waychunas et al. 2005, Nassar 2012), than their larger-sized counterparts of natural origin. This brings about increasing synthesis costs if this clean-up technology is desired for large-scale operations.

In the present work, we investigated the surface reactivity of natural and synthetic magnetites of different particle sizes towards aqueous Pb(II) and Zn(II). These magnetites

were previously characterized and shown to be composed of large and tight aggregates of smaller nanoparticles (Rivas et al. 2006, Rivas et al. 2009, Salazar et al. 2013). Strong inner-sphere interactions are expected at the magnetite-water interface with Pb(II) and Zn(II) ions, based on their reactivity towards other iron oxides such as goethite, hematite and ferrihydrite (Bargar et al. 1997, Waychunas et al. 2002), making it a potentially important process of Pb(II) and Zn(II) ions removal from natural and engineered environments.

In part I of the present series (Salazar et al. 2013) we characterized the natural and synthetic magnetites used in the present work, and investigated their As(V) adsorption behavior as related to the their surface characteristics and particle aggregation behavior. In the present work (part II of the series), maximum adsorption capacities and adsorption kinetics of Pb(II) and Zn(II) on the same magnetite aggregates were investigated, with the goal of evaluating their potential use as adsorbent materials for environmental remediation purposes.

MATERIALS AND METHODS

Reagents and materials

Pb and Zn stock solutions were prepared using Pb(II) and Zn(II) high purity standard solutions of 1000 mg/L in 2 % HNO_3. All chemicals used in this study were reagent grade and were used without additional purification. Sodium hydroxide (NaOH) and nitric acid (HNO_3) were used to adjust pH for all experiments, and sodium nitrate ($NaNO_3$) was used to adjust ionic strength. All these chemicals reagents were purchased from J.T. Baker and Sigma Aldrich, respectively. Deionized water of 17.2 Ω cm conductivity was used in all experiments.

The natural magnetite samples used were obtained from the Peña Colorada iron ore deposit located in the Colima State, in Central-Western Mexico. Two additional commercial (from Sigma Aldrich) synthetic magnetite samples were used as reference materials.

A detailed characterization of all magnetite samples used is described in a previous work (Salazar et al. 2013). Briefly, based on their Fe contents natural samples were determined to be composed of highly-pure magnetite (95-99 %, similar to commercial samples). Their surfaces showed small impurities of aluminosilicates, which decreased their isoelectric points by several pH units from those of synthetic magnetites (6.2-6.7; **Table I**). Very few impurities of goethite and hematite were detected at their surfaces through surface RAMAN spectroscopy. The specific surface area (SSA) values ranged from 1 to 8 m^2 /g, for natural samples, and were 7.3 m^2 /g for the labeled "< 5 mm" synthetic sample, and 39.3 m^2 /g for the "< 50 nm" synthetic sample. X-ray diffraction (XRD) and transmission electron microscopy (TEM) analyses showed that coarser natural samples were composed of aggregated particles/crystallites of 48–52 nm, 39 nm for a finer natural sample (948-fine), 41 nm for sample < 5 μm and 20 nm for sample < 50 nm (**Table I**). Scanning electron microscopy (SEM) and dynamic laser scattering (DLS) studies showed that finer samples have the widest size distribution patterns of aggregates among samples, with mean values of 7, 3 and 98 μm for 948-fine, < 5 μm and < 50 nm samples, respectively. Although the larger aggregates of the smallest sized sample are apparently comprised of open dynamic frameworks. SEM images of coarser samples showed a similar distribution and a mean value of 38 μm as tightly-bound aggregate.

TABLE I
PHYSICAL AND CHEMICAL CHARACTERIZATION PARAMETERS OF MAGNETITES INVESTIGATED

Sample	Sample origin	SSA (m^2/g)	Crystal size (nm)	Aggregated particle average size in suspension (mm)	Isoelectric point
<50 nm	Synthetic	39.3	20	98	6.7
<5 mm	Synthetic	7.3	41	3	6.2
948-fine	Natural	7.6	39	7	4.2
948	Natural	3.0	48	32	3.1
996	Natural	1.4	52	38	<2.0

SSA Specific surface area

Adsorption experiments and analytical methods

We chose for adsorption experiments only two of the coarser natural samples, 996 and 948, as representative of the behavior of the four samples available; and the three finer samples (natural 948fine, and synthetic < 5mm, and < 50 nm). All adsorption experiments were performed under surface saturation conditions and as a function of contact time. They were conducted in batch, in teflon containers of 250 mL at room temperature. The suspensions were prepared in aqueous solutions that contained 0.01M $NaNO_3$ and initial concentrations of Pb(II) of 97 mmol/g for samples 948 and 948-fine, 19 mmol/g for sample 996, 322 mmol/g for sample < 50 nm and 193 mmol/g for sample < 5 mm. The magnetite solids concentrations were 0.3 g/L for sample < 50 nm, 0.50 g/L for < 5 mm, 948 and 948-fine, and 2.6 g/L for 996. For Zn(II), initial concentrations were 612 mmol/g for sample < 50 nm, 312 mmol/g for sample < 5 mm and 44 mmol/g for samples 948, 948-fine and 996, and the magnetite solids concentration were 0.25 g/L for sample < 50 nm, 0.49 g/L for < 5 mm and 3.5 g/L for 948, 948-fine and 996. Solutions and suspensions were prepared weighing the reagents and the magnetite solid in the teflon containers. The experiments were fixed at pH 5.8 for Pb(II) and 7.0 for Zn(II) by adding, with a dropper, small amounts of dilute solutions of NaOH and HNO_3 1.0, 0.1 and 0.01 M, respectively. These pH values were chosen as the maxima before the respective hydroxy/carbonate minerals form (see Results section). Suspensions with magnetite, $NaNO_3$ and Pb(II) or Zn(II), were shaken at 240 rpm using an orbital shaker. At appropriate times between 1 and 110 days for Pb, and 2 and 36 days for Zn, aliquots of 10 to 20 mL of suspension were extracted using plastic syringes and filtered using holder-filters Swinnex and Millipore cellulose membrane filters of 0.05 mm pore size. Finally, the filtrates were stored in polypropylene containers, acidified with 60 mL of HNO_3 for every 10 mL of sample and kept refrigerated (no more than 2 days) until analysis. Aqueous Pb and Zn contents in the filtrates were determined by atomic absorption spectroscopy (AAS). For this, standards solutions between 1 and 10 mg/L for Pb(II) and 0.1 and 1.0 mg/L for Zn(II) were prepared using 1000 mg/L stock solutions. All standards were acidified with 60 mL of concentrated HNO_3 for each 10 mL of standard. The adsorbed Pb and Zn concentrations were calculated by subtracting the final aqueous concentrations measured, from the initially added concentrations.

Analytical methods and equipments used

Pb(II) and Zn(II) concentrations in aqueous solution were measured using a Varian SpectraAA 110 Atomic Absorption equipment, at a wavelength of 283.3 nm for Pb and 213.9 for Zn, using a mixture of 3.5 L/min of air and 1.5 L/min of acetylene. The pH measurements in all experiments were performed with a Beckman 350 pHmeter. The Metrohm glass electrode used was calibrated at 25 °C using J. T. Baker buffer solutions of pH 4, 7 and 10.

Adsorption kinetic models

Three simple models, pseudo-first-order, pseudo-second-order and intraparticle diffusion were applied to test for best fit of adsorption data.

Pseudo-first order kinetic model

The Lagergren model was the first rate equation (Lagergren 1898) applied for the adsorption of a solute in a liquid-solid system, based on the maximum adsorption capacity. It assumes that the rate of change of adsorbate uptake with time is directly proportional to the difference in the saturation concentration and the amount of solid uptake with time. The equation used to fit the adsorption data of Pb and Zn to the pseudo-first order kinetics, has the form of equation (1).

$$\frac{dq_t}{d_t} = k_1 (q_e - q_t) \quad (1)$$

where k_1 is the pseudo-first order adsorption rate coefficient, qe represents the maximum concentration of Pb or Zn adsorbed per unit mass of adsorbent at equilibrium, and qt the concentration adsorbed at any time t. To obtain the value of k1 the integrated form of equation (1) was used for the boundary conditions of t = 0, qt = 0, and t = t, qt = qt (Eq. 2). The value of k1 was obtained from the slope of the linear plot of ln(qe – qt) vs t. To fit adsorption data to this model, according to equation (2), the value of qe must be known.

$$Ln\,(q_e - q_t) = Lnq_e - k_1 t \quad (2)$$

According to Azizian (2004) the observed rate constant (k_1) is a combination of adsorption (ka) and desorption (kd) rate constants. Also, the rate constant (k_1) is a linear function of the initial concentration of solute.

Pseudo-second order kinetic model

Since the pseudo-first order equation (2) did not fit well the adsorption rate, a pseudo-second order kinetics model was tested, on the basis of equation (3) (Ho and McKay 1998a,b). This equation, based on the amount of sorbate, has the form

$$\frac{dq_t}{d_t} = k_2 (q_e - q_t)^2 \quad (3)$$

where qt and q_e, as mentioned before, represent the concentrations of Pb or Zn adsorbed at any time t and the maximum adsorbed per unit mass of adsorbent at equilibrium, respectively, and k_2 is the rate constant of the pseudo-second order adsorption. To obtain the value of k_2, separation of the variables of equation (3) was made followed by integration and application of the same boundary conditions as before (qt = 0 at t = 0 and qt = qt at t = t), yielding the integrated rate law for pseudo-second-order reaction

$$\frac{1}{(q_e - q_t)} = \frac{1}{q_e} + k_2 t \quad (4)$$

Equation (4) can be rearranged to obtain a linear form.

$$\frac{t}{q_t} = \frac{1}{k_2\, q_e^2} = \frac{1}{q_e} t \quad (5)$$

Equation (5) predicts that the ratio of the time/adsorbed concentration of Pb or Zn at any time t should be a linear function of time. qe and k_2 can be obtained experimentally from the

slope and intercept of a plot of t/q_t vs. t, if the plot yields a linear relationship (Rudzinski and Plazinski 2009). According to Azizian (2004), the rate constant is a complex function of the initial concentration of solute.

Intraparticle diffusion kinetic model

According to Weber and Morris (1963), if the rate of sorption is controlled by intraparticle diffusion kinetics a plot of solute sorbed against square root of contact time should yield a straight line passing through the origin. If not, it is likely that intraparticle diffusion is not the only process involved in the adsorption kinetics. The most widely applied equation by Weber and Morris for intraparticle diffusion, has the form

$$q_t = k_1 t^{0.5} \quad (6)$$

where k_1 is the diffusion rate coefficient.

RESULTS AND DISCUSSION

Speciation of aqueous and solid Pb(II) and Zn(II) as a function of pH

The pH of the aqueous solution is an important controlling parameter in heavy metal adsorption processes because high values promote an increase in the concentration of negatively-charged surface groups of adsorbents, thus increasing cation adsorption and decreasing anion adsorption. Before performing cationic heavy metal adsorption experiments it is necessary to determine the upper working pH limit before hydroxy-and/or carbonate solids of the metals (II) precipitate out. Speciation of these ions was performed with the computer program MINEQL+ version 4.5 (Schecher and McAvoy 2001). **Figures 1** and **2** show the speciation of Pb(II) and Zn(II), respectively at the total concentrations used in the adsorption experiments. Solids form above pH 6.1 for Pb(II) [$Pb(OH)_2$ and hydrocerrusite - $Pb_2(CO_3)_2(OH)_2$], and above pH 7.4 for Zn(II) [two types of ZnO]. These pH values are related to the saturation indices (SI), which are plotted in the ordinates of **figures 1** and 2. The saturation index is a useful parameter to determine the degree of saturation of a solution with respect to a given mineral; and it is defined as shown in equation (7),

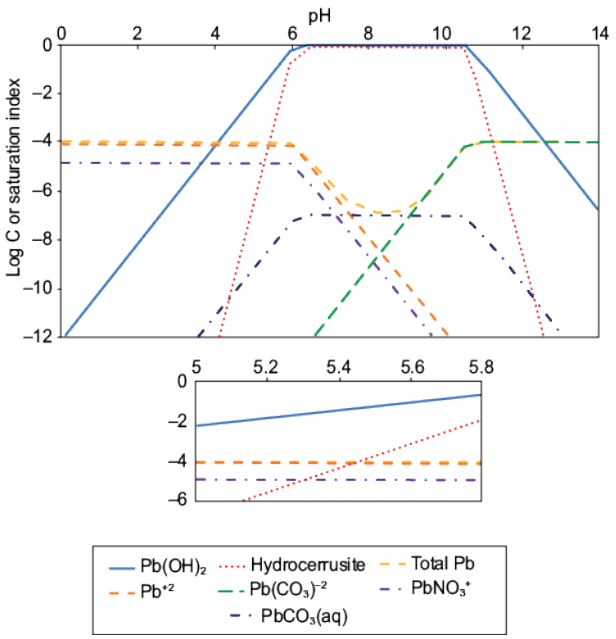

FIG. 1
Speciation of Pb(II) in aqueous solution at an initial Pb(II) concentration of 96.5 µmol/L, $NaNO_3$ of 0.01 M and Log PCO2 of −3.5

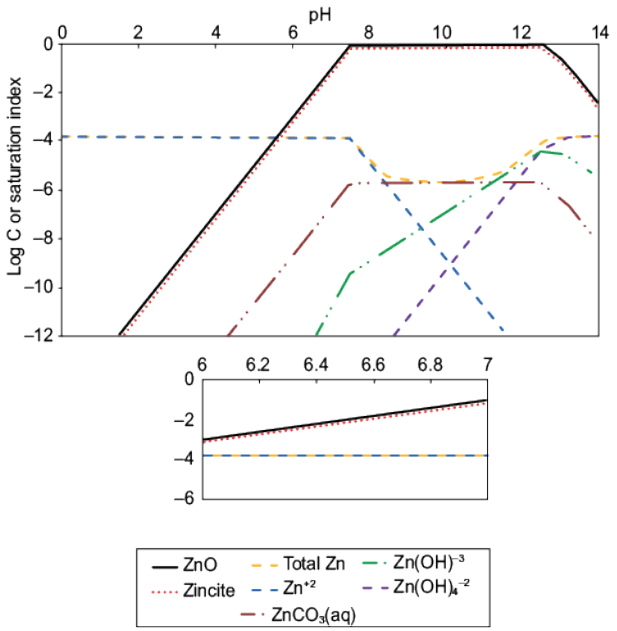

FIG. 2
Speciation of Zn(II) in aqueous solution at an initial Zn(II) concentration of 153 µmol/L, $NaNO_3$ of 0.01 M and Log PCO2 of −3.5

$$SI = Log_{10}\left(\frac{IP}{K_{sp}}\right) \quad (7)$$

where IP is the ionic product and K_{sp} is the solubility product constant of the minerals. At the pH value in which SI is zero ($IP = K_{sp}$) the solution is saturated, so the solid phases may begin to appear. Based on these, to ensure conditions for maximum adsorption for cations before solids formation, the working pH values chosen were 5.8 for Pb(II) and 7.0 for Zn(II). At these values, the predominant dissolved species expected are: Pb^{+2}, $Pb(CO_3)^{-2}$, $PbNO_3$+ and $PbCO_3$(aq); and Zn^{+2}, $Zn(OH)^{-3}$, $Zn(OH)_4^{-2}$ and $ZnCO_3$(aq) for Pb(II) and Zn(II), respectively.

Pb(II) adsorption vs. time

Pb(II) adsorption data as a function of time on natural and synthetic magnetite samples, normalized by mass and SSA, are shown in figures **3a** and **b**, respectively. Retention values per mass showed a direct relation with SSA (Fig. 3a), except for 948-fine, which readily surpassed < 5 mm almost from the beginning. After approximately 40 days the trend was also broken by coarser sample 948, which surpassed < 5 mm. Adsorption equilibrium was reached faster for the finer samples (5, 13 and 38 days for samples < 5 mm, < 50 nm and 948-fine, respectively) than for the coarser ones, especially for 948, which after 110 days does not appear to have reached stable values. This behavior is unusual because in larger particles, in theory the fewer available surfaces sites should be occupied more rapidly.

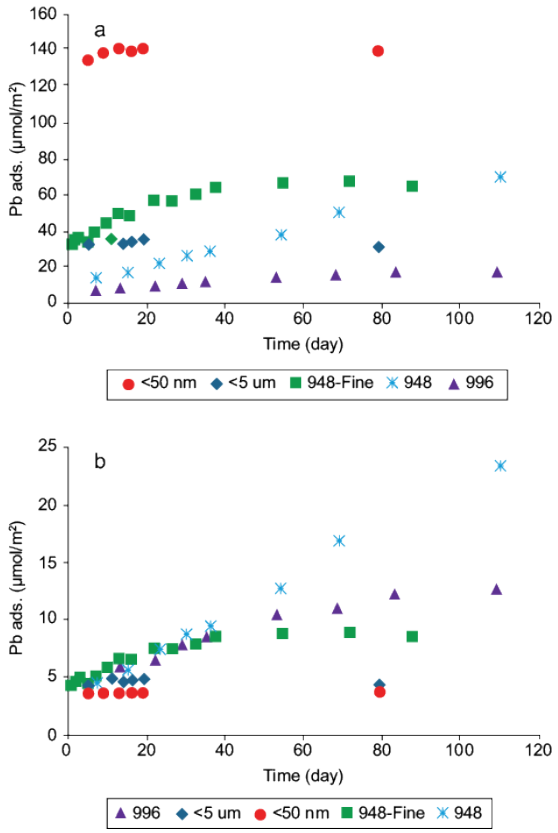

FIG. 3
Adsorption of Pb(II) vs. time on magnetite normalized by (a) mass, (b) specific surface area. The experimental conditions were: [Pb]o = 97 µmol/g for samples 948 and 948-fine, 19 µmol/g for sample 996, 322 µmol/g for sample < 50 nm and 193 µmol/g for sample < 5 µm. The pH was 5.8 in all experiments and the solids concentration was 0.3 g/L for sample < 50 nm, 0.50 g/L for < 5 µm, 948 y 948-Fine and 2.6 g/L for 996. Pb ads. on the y-axis represents the amount of adsorbed lead per unit of mass and area

This behavior might be associated with slow diffusion of Pb(II) into magnetite aggregates, especially in sample 948. Pb diffusion in amorphous iron oxides HFO ($Fe_2O_3 \cdot nH_2O$, n= 1–3) for periods that exceed 110 days has been reported by other authors (Fan et al. 2005, Xu et al. 2006). These authors reported that Pb(II) adsorption on HFO at pH 5.0 could be described by a two-step process: a fast initial adsorption of metal ion to the external surface, followed by a slow intraparticle diffusion step represented by a surface diffusivity of 2.5×10^{-15} cm^2/s.

When data were normalized by SSA (Fig. 3b) neither congruency between adsorption data nor grouping around similar values of SSA and solid concentrations were obtained for magnetite samples. This behavior may be due to an artifact in the BET-SSA measurements, since these are performed in dry samples, in which magnetism might cause considerable and variable aggregation of particles. This aggregation under dry conditions may occur in different forms than in suspended samples, resulting in an incorrect measurement of this parameter when applied to aqueous suspension conditions. However, it is noteworthy that maximum adsorption normalized by SSA is directly correlated to particle size, suggesting that errors in SSA measurements are larger in the coarser magnetite samples. In this regard, the synthetic and smaller particles sized magnetites (< 50 nm and < 5 mm) yielded the lowest maxima computed (3.6 $mmol/m^2$ and 4.8 $mmol/m^2$, respectively), but closer to values shown for maximum anion adsorption on other Fe(III) oxides, such as goethite. The maxima for the remaining natural samples are extremely high and definitely suggest significant underestimation of available SSA.

Another possible contributor to the high and slow adsorption behavior in natural samples may be the presence of clay mineral impurities as is reported previously by SEM-EDS and XRD, which are apparently relatively concentrated on the natural magnetite surfaces (Salazar et al. 2013). Slow Pb(II) diffusion into the structures of these clay impurities may contribute to the slow equilibration shown.

Zn(II) adsorption vs. time

In the case of Zn(II) adsorption normalized by magnetite mass (Fig. 4a), the values are directly related to SSA across the whole time interval studied. All samples showed a similar

variability with time, and therefore better grouping around similar SSA values than in the case of Pb(II) (Fig. 3a). Also, natural samples reached equilibrium faster, but have considerably lower Zn(II) adsorption maxima than for Pb(II). The value of the hydrated radius of Zn(II) (4.30 Å) is larger than that of Pb(II) (4.01 Å) (Volkov et al. 1997, Giraldo et al. 2013) and therefore it is possible that the smaller hydrated Pb(II) reaches sites in natural magnetites inaccessible to Zn(II) (e. g., clay interlayer sites as magnetite impurities), requiring longer times to reach equilibrium. Conversely, for synthetic samples equilibrium was reached more rapidly for Pb(II) (Fig. 3a) than for Zn(II) (Fig. 4a), despite the fact that the adsorption maxima were similar. This suggests that Pb(II) has a greater adsorption affinity towards magnetite surface sites than Zn(II), which most probably bind as inner sphere surface complexes, i. e., without their hydration sphere.

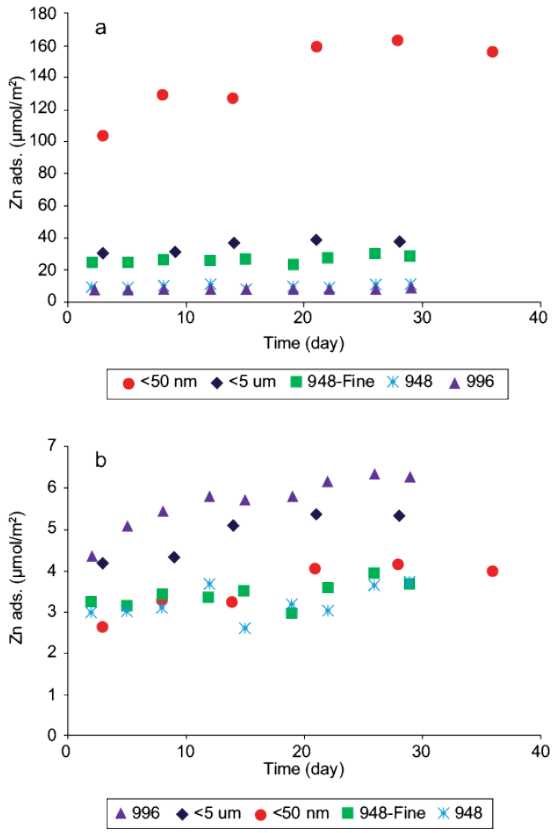

FIG. 4
Adsorption of Zn(II) vs. time on magnetite normalized by (a) mass, (b) specific surface area. The experimental conditions were: [Zn]o = 612 µmol/g for sample < 50 nm, 312 µmol/g for sample < 5 µm and 44 µmol/g for samples 948, 948-fine and 996. The pH was 7.0 in all experiments and the solids concentration was 0.25 g/L for sample < 50 nm, 0.49 g/L for < 5 µm and 3.5 g/L for 948, 948-fine and 996. Zn ads. on the y-axis represents the amount of adsorbed zinc per unit of mass and area

When Zn(II) adsorption data were normalized by SSA (Fig. 4b) a remarkable adsorption congruency was observed for samples 948, 948-fine, and < 50 nm, with maxima between 3 and 4 mmol/m^2, which are physically realistic values for adsorption on iron oxides. Samples < 5 mm and 996 showed considerably higher adsorption values, but not nearly as high as those shown by Pb(II) (Fig. 3b). Again, this may be explained by underestimated SSA from high aggregation under dry conditions, but the large difference in behavior between the two coarser samples, 948 and 996, is not clear, especially because the trend is opposite to that shown by Pb(II).

Adsorption kinetic models

Most of the adsorption/desorption processes on various solids phases are time-dependent, especially for heterogeneous compositions. To understand the interaction of contaminants such as Pb(II) and Zn(II) in solution with reactive mineral phases when adsorption processes dominate their mobility, and in general to predict their fate with time, it is important to determine the kinetic parameters involved (Sparks 1989, Sparks and Suárez 1991). Such parameters were determined using pseudo-first and pseudo-second order models. According to Azizian (2004), when the initial amount of solute in solution is high compared with the amount of solute that can be sorbed by the solid, pseudo-first-order model is suitable for analysis of sorption kinetics, and when the initial amount of solute is comparable with the sorption capacity of the solid, then the pseudo-second-order model becomes suitable to fit the data. The nature of sorption process will depend on physical or chemical characteristics of the adsorbent and on the system conditions.

Comparison of correlation coefficients (R) of the linearized forms of both rate equations applied to the experimental adsorption data indicates that their behavior followed a pseudo-second order kinetic model (**Table II**). R values for both metals were 0.99 or higher for all magnetites, except for sample 948 (T**able II**), which yielded R values of 0.855 for Pb(II) and 0.972 for Zn(II). Also, for this latter sample, it was not possible to fit a pseudo-first order kinetic model because the concentration of Pb adsorbed was nowhere near equilibrium after 110 days, and thus qe was unknown.

TABLE II
LINEARIZATION OF KINETIC MODELS APPLIED TO THE ADSORPTION DATA OF Pb(II) AND Zn(II) ON NATURAL AND SYNTHETIC MAGNETITES

Lead					
Samples	Pseudo-first order	Pseudo-second order			
	R	k_2 (g/µmol/min)	$q_{e\ exp}$ (µmol/g)	$q_{e\ cal}$ (µmol/g)	R
<50 nm	0.815	0.422	140.1	140.9	1.000
<5 mm	0.725	0.093	33.3	31.0	1.000
948-Fine	0.936	0.012	65.4	69.0	0.998
996	0.943	0.007	17.0	20.6	0.990
948	-	-	-	-	0.855
Zinc					
<50 nm	0.694	0.023	159.2	172.4	0.995
<5 mm	0.947	0.048	38.8	41.2	0.998
948-Fine	0.730	0.096	28.2	28.5	0.985
996	0.921	0.237	8.5	9.0	0.999
948	0.578	0.192	11.0	10.8	0.972

$q_{e\ cal}$: Calculated c
oncentration of Pb and Zn adsorbed normalized by adsorbent mass at equilibrium
$q_{e\ exp}$: Experimental concentration of Pb and Zn adsorbed normalized by adsorbent mass at equilibrium
k_2 : Rate constant of pseudo-second order
R: Regression coefficient

The excellent fits to pseudo-second order models for the entire adsorption range of the different samples is expected, since the adsorption range investigated reaches full saturation of sites on the magnetite surfaces. It has been shown through spectroscopic studies that Pb(II) and Zn(II) bind to the surface of other iron oxides forming inner-sphere complexes (Bargar et al. 1997, Ostergren et al. 2000, Lenhart et al. 2001, Trivedi et al. 2003, 2004, Lee and Anderson 2005), so it is likely that these ions also bind covalently to magnetite. Also, the kinetics of adsorption of Pb and Zn onto various adsorbents, included magnetite, has been found to follow a pseudo-second order kinetics (Gupta and Bhattacharyya 2011, Shahmohammadi et al. 2011, Kumari et al. 2015).

The calculated values of equilibrium capacities ($q_{e\ cal}$) from the pseudo-second order model were very close to the experimentally obtained capacities ($q_{e\ exp}$) (Table II). Also, confirming the experimental observations, the pseudo-second order rate constants (k_2) obtained for Pb(II) were higher than for Zn(II) in synthetic samples,

while the opposite was obtained for natural samples. This indicates that Pb(II) has a higher affinity toward magnetite than Zn(II), while for natural samples Pb(II) diffusion into impurities was likely responsible for the slower adsorption behavior, because of its smaller hydrated radius and thus accessibility to sites that are likely diffusion-dependent, as was mentioned earlier.

To verify that Pb(II) diffusion into natural samples may contribute to the slow equilibration shown, an intraparticle diffusion model was tested, based on equation (6). From table III it can be seen that for this metal natural samples had good linearity (regression coefficient, R ≥ 0.98) and the intraparticle diffusion coefficients for samples 948-fine, 996 and 948 had values of 6.2, 1.5 and 7.3 mmol/g/day, respectively. Also, table III shows that the plot of Pb adsorbed against square root of contact time did not have a zero intercept. This last result indicates that in addition to following intraparticle diffusion (e.g. in magnetite impurities), pseudo-second-order kinetics might also be a process influencing the kinetics of natural samples (Gupta and Bhattacharyya 2011). A similar result was reported by Sari et al. (2007), in a study of adsorption of Pb(II) on Turkish kaolinite.

TABLE III
INTRAPARTICLE DIFFUSION KINETIC MODEL PARAMETERS FOR Pb(II) AND Zn(II) ION ADSORPTION ONTO NATURAL MAGNETITE SAMPLES

Samples	Lead			Zinc	
	R	k_i (μmol/g/day$^{0.5}$)	Intercept (μmol/g)	R	k_i (μmol/g/day$^{0.5}$)
948-Fine	0.983	6.171	24.454	0.594	0.958
996	0.991	1.455	2.812	0.967	0.659
948	0.979	7.323	–11.732	0.460	0.392

R: Regression coefficient
k_i : Diffusion rate coefficient

In the case of Zn(II), natural samples had low linearity (regression coefficient, R ~ 0.46 to 0.60), except the sample 996. Nevertheless, intraparticle diffusion coefficients are very low (0.39 to 0.96, table III), so that the contribution of diffusion on the kinetics of Zn(II) adsorption on natural samples would be also very low.

We should note that another possible sorption mechanism of divalent heavy metal ions under high loading conditions is through formation of olygomeric or multinuclear species at the surface, especially for Pb(II), which may also show slow formation kinetics. But, regardless of the specific mechanisms involved, the total metal sorption capacities for the finer magnetite samples are quite high.

Comparison with previous work and implications of magnetite Pb(II) and Zn(II) adsorption capacities

Previous Pb(II) adsorption work on magnetite nanoparticles with average sizes from 8 to 60 nm (Table IV), has shown equilibrium times achieved within the first 20-600 minutes of the experiments (Wang et al. 2011, Giraldo et al. 2013, Karami 2013, Wang et al. 2014). These times are considerably shorter than the times obtained with our natural magnetite samples, presumably because of the extremely high surface area exposed in nanoparticles, which allows fast diffusion of the ions from the bulk solution to the nanomagnetite surfaces (Nassar 2010, Wang et al. 2011).

TABLE IV
ADSORPTION CAPACITIES OF Pb(II) AND Zn(II) ON MAGNETITES FROM THE LITERATURE

Metal	Maximum adsorption capacity (μmol/g)	pH	Particle size (nm)	SSA–BET-N_2 (m^2/g)	Reference
Pb	110.5	5.0	10	115.3	Wang et al. 2011
Pb	180.0	5.5	8 -10	95.5	Giraldo et al. 2013
Pb	170.0	5.5	22	39	Nassar 2010[a]
Pb	113.0	5.5	55-65	-	Karami 2013[b]
Pb	64.5	5.0	150-250	11.3	Kumari et al. 2015[c]
Pb	16.6	3.8	15	125.8	Wang et al. 2014[d]
Zn	285.0	7.0	10-15	103.0	Iwahori et al. 2014
Zn	9.5	7.0	-	5.4	Iwahori et al. 2014
Zn	160.0	5.5	8 -10	95.5	Giraldo et al. 2013
Zn	107.0	5.5	55-65	-	Karami 2013[b]

SSA-BET-N_2 Specific surface area determined by nitrogen adsorption

[a] External SSA. Estimated SSA 43 m^2 /g, average pore volume 0.38 cm^3 /g

[b] Nanorods with diameters of ca. 55-65 nm and lengths of 900-1000 nm. Obtained from transmission electron microscopy images

[c] Mesoporous nanospheres with average size of 150 -250 nm in diameter, hollow cavities of 90-160 nm in diameter and an average individual nanoparticle size of 31.2 nm

[d] Initial pH. In this experiments pH was not adjusted

A comparison of adsorption maxima also shows higher values for nanomagnetites (Table IV), and thus comparable to our < 50 nm sample (141 mmol/g – Fig. 3). Larger particle/aggregate sizes, heterogeneities and low specific surface areas in natural magnetite samples and in sample < 5 mm explain the slower adsorption and lower maxima (2 to 9 fold lower – **Tables II** and **IV**). Although sample < 50 nm showed large aggregates (average of 98 mm – Salazar et al. 2013), its adsorption capacity was considerably higher than those of the other samples, with smaller average aggregate sizes. This supports the hypothesis that the aggregates formed by the < 50 nm magnetite have an open and dynamic structure, that do not block to a large extent the available surface area of individual particles. The low Pb(II) adsorption value of 17 mmol/g reported for a 15 nm magnetite sample (Table IV) was due to the lower pH investigated of 3.8, in which protons are exerting a stronger competition against Pb(II) adsorption.

In the case of Zn(II) adsorption onto magnetite, a comparison with previous work is possible with a larger-sized synthetic sample of 5.4 m^2 /g, which adsorbed a maximum of 9.5 mmol/g at pH 7 (Iwahori et al. 2014 - **Table IV**). This value is closer to those of our coarser magnetite samples (Table II), but considerably smaller than those of our finer synthetic and natural samples of similar SSAs (7.3 and 8 m^2 / g, respectively). As in the case for Pb(II), smaller nanomagnetites (10-15 nm) than ours (< 50 nm) yielded considerably larger Zn(II) adsorption maxima (285 mmol/g – **Table IV** , vs. 172 mmol/ g – **Table II**). Finally, Zn(II) adsorption maxima reported at pH 5.5 are not directly comparable to ours, and evidently yield lower values to our magnetites of comparable sizes.

Judging from adsorption capacity comparisons, our results showed that for practical purposes, samples < 50 nm, < 5mm and 948-fne, can be considered as efficient adsorbents and can be applied in water treatment systems for removal of Pb(II) and Zn(II), and probably other metal(II) cations, at pH values that are environmentally relevant. Additionally, they can be used to decontaminate soil and heterogeneous solids since magnetite allows for magnetic separation of the adsorbed contaminants from the matrix.

CONCLUSIONS

In this work, the rates and capacities of natural and synthetic magnetites for removing Pb(II) and Zn(II) ions from aqueous solutions were evaluated. No congruency of maximum Pb(II) and Zn(II) adsorption data was obtained when data were normalized by mass or by SSA, with no clear trends observed either. This behavior was assumed to be the result of variable aggregation states of the magnetic particles in the different samples, which may cause important underestimations of available SSA to

different degrees, especially for the magnetites of larger particle sizes. Also, Pb(II) adsorption equilibrium in natural samples was found to occur at considerably longer time than previous studies on synthetic magnetite nanoparticles. The pseudo-second order rate model showed a very good description of the Pb(II) and Zn(II) adsorption kinetics data. However, intraparticle diffusion [especially in Pb(II) case] also appears as an important contributor in the adsorption process of natural samples, which may explain the longer times to reach equilibrium in these samples, as compared to the synthetic ones.

Finally, the results showed that for practical purposes, synthetic samples < 50 nm, < 5 mm and natural sample 948-fine, can be used as efficient Pb(II) and Zn(II) adsorbents in treatment systems of contaminated water and soil, at pH values that are environmentally relevant.

Acknowledgements

C.S.-C is grateful to the CONACyT for the Doctoral's student grant provided and to Katherine Vaca-Escobar for providing guidance in the use of MINEQL for aqueous speciation modeling. The authors are very grateful to the personnel of Laboratorio de Química Ambiental (LABQA) of the Universidad Nacional Autónoma de México (UNAM) for making laboratory space and infrastructure available for the experimental work performed; to the Consorcio Minero Benito Juárez Peña Colorada for providing the natural magnetite samples used in the study, and also to two anonymous reviewers, who helped improve the clarity of the manuscript.

References

Arancibia N., Baltazar S., García A., Muñoz D., Sepúlveda P., Rubio M. and Altbir D. (2016). Nanoscale zero valent supported by Zeolite and Montmorillonite: template effect of the removal of lead ion from an aqueous solution. J. Hazard. Mater. 301, 371-380. DOI: 10.1016/j.jhazmat.2015.09.007

Atar N., Olgun A. and Wang S. (2012). Adsorption of cadmium (II) and Zinc (II) on boron enrichment process waste in aqueous solutions: Batch and fixed-bed systems studies. Chem. Eng. J. 192, 1-7. DOI: 10.1016/j.cej.2012.03.067

ATSDR (2005). Public health statement: zinc. Division of toxicology, U.S. department of health and human services, public health service, Agency for Toxic Substances and Disease Registry. Atlanta, USA, 352 pp.

ATSDR (2012). Public health statement: cadmium. Division of toxicology, U.S. department of health and human services, public health service, Agency for Toxic Substances and Disease Registry. Atlanta, USA, 487 pp.

Azizian S. (2004). Kinetics models of sorption: a theoretical analysis. J. Colloids Interface Sci. 276, 47-52. DOI: 10.1016/j.jcis.2004.03.048

Bargar J., Brown Jr G. and Parks G. (1997). Surface complexation of Pb(II) at oxide-water interface: II. XAFS and bond valence determined of molecular Pb(II) sorption products and surface functional groups on iron oxides. Geochim. Cosmochim. Acta 61, 2639-2652. DOI: 10.1016/S0016-7037(97)00125-7

Bargar J., Brown Jr G. and Parks G. (1998). Surface complexation of Pb(II) at oxide-water interfaces: III. XAFS determination of Pb(II) and Pb(II)-chloro adsorption complexes on goethite and alumina. Geochim. Cosmochim. Acta 62, 193-207. DOI: 10.1016/S0016-7037(97)00334-7

Barquist K. and Larsen C. (2010). Chromate adsorption on bifunctional, magnetic zeolites composites. Micropor. Mesopor. Mat. 130, 197-202. DOI: 10.1016/j.micromeso.2009.11.005

Fan M., Boonfueng T., Xu Y., Axe L. and Tyson T. (2005). Modeling Pb sorption to microporous amorphous oxides as discrete particles and coatings. J. Colloid Interface Sci. 281, 39-48. DOI: 10.1016/j.jcis.2004.08.050

Giraldo L., Erto A. and Moreno J. (2013). Magnetite nanoparticles for removal of heavy metals from aqueous solutions: synthesis and characterization. Adsorption 19, 465-474. DOI: 10.1007/s10450-012-9468-1

Gupta S. and Bhattacharyya K. (2011). Kinetics of adsorption of metal ions on inorganic materials: A review. Adv. Colloids Interface Sci. 162, 39-58. DOI: 10.1016/j.cis.2010.12.004

Ho Y. and McKay G. (1998a). A comparison of chemisorptions kinetic models applied to pollutant removal on various sorbents. Process Saf. Environ. Prot. 76, 332-340. DOI: 10.1205/095758298529696

Ho. Y. and McKay G. (1998b). The kinetics of sorption of basic dyes from aqueous solution by Sphagnum moss peat. Can. J. Chem. Eng. 76, 822-827. DOI: 10.1002/cjce.5450760419

Hua M., Zhang S., Pan B., Zhang W., Lu L. and Zhang Q. (2012). Heavy metal removal from water/wastewater by nanosized metal oxides: A review. J. Hazard. Mater. 211-212, 317-331. DOI: 10.1016/j.jhazmat.2011.10.016

Iwahori K., Watanabe J., Tani Y., Seyama H. and Miyata N. (2014). Removal of heavy metal cations by biogenic magnetite nanoparticles produced in Fe(III)-reducing microbial enrichment cultures. J. Biosci. Bioeng. 117, 333-335. DOI: 10.1016/j.jbiosc.2013.08.013

Karami H. (2013). Heavy metal removal from water by magnetite nanorods. Chem. Eng. J. 219, 209-216. DOI: 10.1016/j.cej.2013.01.022

Kong X., Han Z., Zhang W., Song L. and Li H. (2016). Synthesis of Zeolite-supported microscale zero-valent iron for the removal of Cr+6 and Cd +2 from aqueous solution. J. Environ. Manage. 169, 84-90. DOI: 10.1016/j.jenvman.2015.12.022

Kumari M., Pittman Jr C. and Mohan D. (2015). Heavy metals [chromium (VI) and lead (II) removal from water using mesoporous magnetite (Fe3O4) nanospheres. J. Colloids Interface Sci. 442, 120-132. DOI: 10.1016/j.jcis.2014.09.012

Lagergren S. (1898). Zur theorie der sogenannten adsorption geloster stoffe, K. Sven. Vetenskapsakad. Handl. 24, 1-39

Lee S. and Anderson P. (2005). Exafs study of Zn sorption mechanism on hydrous ferric oxide over extended reaction time. J. Colloids Interface Sci. 286, 82-89. DOI: 10.1016/j.jcis.2005.01.005

Lenhart J., Bargar J. and Davis J. (2001). Spectroscopic evidence for ternary surface complexes in the lead(II) – malonic acid – hematite system. J. Colloids Interface Sci. 234, 448-452. DOI: 10.1006/jcis.2000.7345

Mudhoo A., Garg V. and Wang S. (2012). Removal of heavy metals by biosorption. Environ. Chem. Lett. 10, 109-117. DOI: 10.1007/s10311-011-0342-2

Nassar N. (2010). Rapid removal and recovery of Pb(II) from wastewater by magnetic nanoadsorbents. J. Hazard. Mater. 184, 538-546. DOI: 10.1016/j.jhazmat.2010.08.069

Nassar N. (2012). Kinetics, equilibrium and thermodynamic studies on the adsorptive removal of nickel, cadmium and cobalt from wastewater by supermagnetic iron oxide nano-adsorbents. Can. J. Chem. Eng. 90, 1231-1238. DOI: 10.1002/cjce.20613

Ostergren J., Trainor T., Bargar J., Brown Jr G. and Parks G. (2000). Inorganic ligand effects on Pb(II) sorption to goethite (a-FeOOH): I. Carbonate. J. Colloids Interface Sci. 225, 466-482. DOI: 10.1006/jcis.1999.6701

Rivas M., Alva L., Arenas J., Urrutia J., Ruiz M. and Ramos M. (2006). Berthierine and chamosite hydrothermal: genetic guides in the Pena Colorada magnetite-bearing ore deposit, Mexico. Earth Planets and Space 58, 1389-1400. DOI: 10.1186/BF03352635

Rivas M., Alva L., Arenas J., Urrutia J., Perrin M., Goguitchaichvili A., Ruiz M. and Molina M. (2009). Natural magnetite nanoparticles from an iron-ore deposit: size dependence on magnetic properties. Earth Planets and Space 61, 151-160. DOI: 10.1186/BF03352895

Rudzinski W. and Plazinski W. (2009). On the applicability of the pseudo-second order equation to represent the kinetics of adsorption at solid/solution interfaces: a theoretical analysis based on the statistical rate

theory. Adsorption 15, 181-192. DOI: 10.1007/s10450-009-9167-8

Salazar C., Villalobos M., Rivas M., Arenas J., Alcaraz J. and Gutiérrez M. (2013). Characterization and surface reactivity of natural and synthetic magnetites. Chem. Geol. 347, 233-245. DOI: 10.1016/j.chemgeo.2013.03.017

Sánchez M., Marmolejo A., Magallanes V. and Sánchez A. (2013). Vertical accumulation of potencial toxic elements in a semiarid system that is influenced by an abandoned gold mine. Estuarine, Coastal and Shelf Science 130, 42-53. DOI: 10.1016/j.ecss.2013.03.017

Sari A., Tuzen M., Citak D. and Soylak M. (2007). Equilibrium, kinetic and thermodynamic studies of adsorption of Pb(II) from aqueous solution onto Turkish kaolinite clay. J. Hazard. Mater. 149, 283-291. DOI: 10.1016/j.jhazmat.2007.03.078

Schecher W. and McAvoy D. (2001). MINEQL+, a chemical equilibrium modeling system. 2a ed. Environmental Research Software, Hallowell, Maine, USA, 164 pp.

Shahmohammadi S., Babazadeh H., Nazemi A. and Manshouri M. (2011). Isotherm and Kinetic Studies on Adsorption of Pb, Zn and Cu by kaolinite. Casp. J. Environ. Sci. 9, 243-255.

Sparks D. (1989). Kinetics of soil chemical processes. Academic Press, San Diego, CA, USA, 222 pp.

Sparks D. and Suárez D. (1991). Rates of soil chemical processes. In: SSSA Special Publications No. 27. Soil Science Society of America, Madison, WI, USA, 296 pp.

Tani Y., Ohashi M., Miyata N., Seyama H., Iwahori K. and Soma M. (2004). Sorption of Co(II), Ni(II), and Zn(II) on biogenic manganese oxides produced by a Mn-oxidizing fungus, strain KR21-2. J. Environ. Sci. Heal. A. 39, 2641-2660. DOI: 10.1081/ESE-200027021

Trivedi P. and Axe L. (2000). Modeling Cd and Zn sorption to hydrous metal oxides. Environ. Sci. Technol. 34, 2215-2223. DOI: 10.1021/es991110c

Trivedi P., Dyer J. and Sparks D. (2003). Lead sorption onto Ferrihidrite. 1. A macroscopic and spectroscopic assessment. Environ. Sci. Technol. 37, 908-914. DOI: 10.1021/es0257927

Trivedi P., Dyer J., Sparks D. and Pandya K. (2004). Mechanistic and thermodynamic interpretations of zinc sorption onto ferrihidrite. J. Colloids Interface Sci. 270, 77-85. DOI: 10.1016/S0021-9797(03)00586-1

Uheida A., Salazar G., Bjorkman E., Yu Z. and Muhammed M. (2006). Fe3O4 and g-Fe2O3 nanoparticles for the adsorption of Co2+ from aqueous solution. J. Colloid Interface Sci. 298, 501-507. DOI: 10.1016/j.jcis.2005.12.057

USEPA (2007). Priority list of hazardous substances. Information center, comprehensive environmental response, compensation, and liability act, Agency for Toxic Substances and Disease Registry. United States Environmental Protection Agency. Atlanta, USA, 6 pp.

Villalobos M., Bargar J. and Sposito G. (2005). Mechanisms of Pb(II) sorption on a biogenic manganese oxide. Environ. Sci. Technol. 39, 569-576. DOI: 10.1021/es049434a

Volkov A., Paula S. and Deamer D. (1997). Two mechanisms of permeation of small neutral molecules and hydrated ions across phospholipid bilayers. Bioelectroch. Bioener. 42, 153-160. DOI: 10.1016/S0302-4598(96)05097-0

Wang T., Jin X., Chen Z., Megharaj M. and Naidu R. (2014). Simultaneous removal of Pb(II) and Cr(III) by magnetite nanoparticles using various synthesis conditions. J. Ind. Eng. Chem. 20, 3543-3549. DOI: 10.1016/j.jiec.2013.12.047

Wang X., Lu H., Zhu L., Liu F. and Ren J. (2011). Adsorption of Lead(II) Ions onto Magnetite Nanoparticles. Adsorpt. Sci. Technol. 28, 5, 407-417. DOI: 10.1260/0263-6174.28.5.407

Waychunas G., Fuller C. and Davis J. (2002). Surface complexation and precipitate geometry for aqueous Zn(II) sorption on ferrihydrite I: X-ray absorption extended fine structure spectroscopy analysis. Geochim. Cosmochim. Acta 66, 1119-1137. DOI: 10.1016/S0016-7037(01)00853-5

Waychunas G., Kim C. and Banfield J. (2005). Nanoparticulate iron oxide minerals in soils and

sediments: unique properties and contaminant scavenging mechanisms. J. Nanopart. Res. 7, 409-433. DOI: 10.1007/s11051-005-6931-x

Weber W. and Morris J. (1963). Kinetics of adsorption on carbon from solution. J. Sanit. Eng. Div. ASCE 89, 31-60.

Xu Y., Boonfueng T., Axe L., Maeng S. and Tyson T. (2006). Surface complexation of Pb(II) on amorphous iron oxide and manganese oxide: Spectroscopic and time studies. J. Colloid Interface Sci. 299, 28-40. DOI: 10.1016/j.jcis.2006.01.041

Funding

Funding source: CONACyT
Award recipient: Los autores